Research article

Identification of novel target molecules of *l*-menthol

Toyoshi Umezu [*]

Health and Environmental Risk Division, National Institute for Environmental Studies, 16-2 Onogawa, Tsukuba, Ibaraki, 305-8506, Japan

ABSTRACT

The present study used a binding assay to identify novel target biomolecules of *l*-menthol ([−]-menthol) that promote mouse ambulation. Among 88 different ligands to specific biomolecules examined, 0.1 mM *l*-menthol inhibited the binding of 13 ligands with relatively high inhibition rates. The assays showed that *l*-menthol acts on calcium channels, sodium channels, γ-aminobutyric acid type A (GABA$_A$) receptor, GABA transporter, dopamine transporter, dopamine D4 receptor, adenosine A2a receptor, α2A-adrenergic receptor, histamine H2 receptor, bombesin receptor, angiotensin AT1 receptor, vasopressin V2 receptor, and leukotriene B4 receptor over a similar concentration range. The inhibition constant (K$_i$) for *l*-menthol inhibition of binding of [^{3}H]-WIN35,428 to the human recombinant dopamine transporter was 6.15×10^{-4} mol/L. The K$_i$ for *l*-menthol inhibition of binding of [^{3}H]-ethynylbicycloorthobenzoate (EBOB), a ligand of GABA$_A$ receptor picrotoxin site, was 2.88×10^{-4} mol/L. These results should aid future research by providing clues for investigating the mechanisms underlying *l*-menthol activities, including the ambulation-promoting effect. The present results suggest that the dopamine transporter, adenosine A2a receptor, dopamine D4 receptor, α2A-adrenergic receptor, and GABA$_A$ receptor are promising candidate molecules that are involved in the mechanisms underlying the psychostimulant-like effect of *l*-menthol.

1. Introduction

Menthol is a cyclic monoterpene alcohol, and is used in a variety of commercial products. Menthol is also used as an additive in foods, beverages, and cigarettes. Medicinal applications of menthol include its use as an enhancer of the cutaneous absorption of medicinal agents, local anesthetics, topical analgesics, antipruritics, and as a gastric sedative (Eccles, 1994; Patel et al., 2007).

The discovery of transient receptor potential melastatin subfamily channel 8 as the target molecule associated with cooling sensation (Peier et al., 2002; McKemy et al., 2002) suggested that specific molecular mechanisms underlay a variety of menthol's activities. Previous studies suggest that menthol acts on a variety of molecules (Oz et al., 2017). These molecules may play roles in various peripheral effects of menthol (Haeseler et al., 2002; Ito et al., 2008; Heimes et al., 2011; Gaudioso et al., 2012; Cheang et al., 2013; Amato et al., 2014). In addition, accumulating evidence indicates that menthol also affects the central nervous system (CNS). In rodents, menthol is distributed throughout the brain after peripheral administration (Pan et al., 2012; Thompson et al., 2018).

Previous studies demonstrated that menthol affects neuronal activity via voltage-gated calcium (Ca) channels (Swandulla et al., 1986, 1987) and acts as an allosteric modulator of serotonin type 3 receptor expressed in neurons (Ashoor et al., 2013). Other studies reported that the γ-aminobutyric acid type A (GABA$_A$) receptor mediates some of the CNS effects of menthol (Zhang et al., 2008; Tani et al., 2010). Moreover, it has been suggested that the CNS effects of menthol play a role in the development of nicotine dependence (Alsharari et al., 2015; Henderson et al., 2016, 2017; Thompson et al., 2018).

Menthol also promotes ambulation in mice (Umezu et al., 2001). The ambulatory effect of menthol is similar to that of psychostimulants but distinct from that of nicotine and CNS depressants (Umezu, 2012, 2013). A study used various dopamine-related pharmacological agents suggests that the dopaminergic nervous system is involved in the ambulation-promoting effect of menthol (Umezu and Morita, 2003). However, the associated target molecules have yet to be identified. Previous studies suggested that the pharmacologically relevant concentration range of menthol is ~0.01–10 mM. The IC$_{50}$ and/or EC$_{50}$ values for menthol with regard to already-identified target molecules are

---

reportedly within the pharmacologically relevant concentration range (Oz et al., 2017). These observations indicate that menthol acts on a variety of different molecules with relatively low specificity. Accordingly, it is possible that menthol also acts on other as yet unidentified biomolecules within the pharmacologically relevant concentration range.

The present study identified novel target biomolecules of menthol. As the major form found in nature is *l*-menthol, the present study examined the effects of this isomer on mouse ambulation and the ability of *l*-menthol to inhibit the binding of 88 different ligands for specific biomolecules to identify potential target molecules of *l*-menthol involved in its ambulation-promoting effect.

2. Materials and methods

2.1. Agents

l-menthol was purchased from Nacalai Tesque (Kyoto, Japan). Positive control substances (Supplementary Table 1) and *l*-menthol were dissolved in dimethyl sulfoxide and then diluted to the final concentrations used in the binding assay.

2.2. Measurement of mouse ambulatory activity

Ambulatory activity was measured using a SAM-10 ambulometer (O'Hara and Co., Tokyo, Japan), which is described in detail elsewhere (Umezu and Shibata, 2016).

The animal experiments were approved by the Committee for Experimental Animals of the National Institute for Environmental Studies, Japan.

2.3. Statistical analysis of ambulatory activity data

To control for differences in baseline ambulatory activity, the ambulatory activity of each mouse was normalized against the total activity of the mouse during the 30-min adaptation period before *l*-menthol administration. Differences in total normalized ambulatory activity were analyzed using the Kruskal-Wallis test, followed by the Wilcoxon test, as the data were not normally distributed. A *P* value of <0.05 was considered indicative of statistical significance.

2.4. Binding assay

A preparation containing the molecule of interest was incubated with a radioactive isotope-labeled ligand, and the quantity of isotope-labeled ligand bound in the absence of positive control substance or *l*-menthol (B_0) was then measured. Nonspecific binding (N) was assessed by incubating the molecule of interest with the radioactive isotope-labeled ligand and a replacement substance (Supplementary Table 1). To measure the quantity of isotope-labeled ligand bound in the presence of positive control substance or *l*-menthol (B), the preparation containing the molecule of interest was incubated with the radioactive isotope-labeled ligand and a positive control substance or 0.1 mM *l*-menthol. After the reactions, the solutions were filtered using filter papers, which were subjected to radioactivity measurement.

The effect of *l*-menthol or positive control on binding of the radioactive isotope-labeled ligand was evaluated using Eq. (1) and Eq. (2):

$$\text{Binding rate} = [(B - N) / (B_0 - N)] \times 100 (\%) \tag{1}$$

$$\text{Inhibition rate} (\%) = 100 - \text{Binding rate} \tag{2}$$

The ability of 0.1 mM *l*-menthol to inhibit the binding of 88 different ligands was examined using the binding assay. Details regarding the preparations containing molecules of interest, radioactive isotope-labeled ligands, positive control substances, and incubation conditions

(e.g., buffer, temperature, and reaction time) examined in this study are shown in Supplementary Table 1.

2.5. Determination of the 50% inhibitory concentration (IC_{50}) and the inhibition constant (K_i) for l-menthol and positive control substances inhibition of the binding of the dopamine transporter ligand [³H]-WIN35,428 and the GABAₐ receptor picrotoxin site ligand [³H]-ethynylbicycloorthobenzoate (EBOB)

The effects of *l*-menthol and GBR12909 at 7 concentrations on [³H]-WIN35,428 binding were evaluated using the binding assay. Similarly, effects of *l*-menthol and picrotoxin on [³H]-EBOB binding were evaluated at 7 concentrations using the binding assay. Given that binding assays are usually performed in duplicate or triplicate, the assay of the present study was duplicated at each concentration as in previous studies (Lever et al., 2017; Mollica et al., 2017; Kaserer et al., 2020), and the mean values were used to determine the IC_{50} for each compound according to Eq. (3), Eq. (4) and Eq. (5). The best-fit equations were determined using a least squares method:

$$Y = aX + b \, (a \text{ and } b \text{ are constants determined by the least squares method}) \tag{3}$$

$$Y = \text{logit } y = \ln(y / 1 - y); \, y = (B - N) / (B_0 - N) \tag{4}$$

$$X = \log x \tag{5}$$

The term x represents the concentration of *l*-menthol or respective positive control substance.

Next, concentration-effect relationships for [³H]-WIN35,428 and [³H]-EBOB binding were evaluated at 7 concentrations of the radio-labeled ligands. The assay was also duplicated at each concentration, and the mean values were used. The equilibrium binding constant (K_d) and maximum specific binding (B_{max}) for [³H]-WIN35,428 and [³H]-EBOB were then determined according to Eq. (6):

$$B / F = - (1 / K_d) \times (B - B_{max}) \tag{6}$$

where B represents the concentration of [³H]-WIN35,428 or [³H]-EBOB corresponding to the bound radioactivity, and F represents the concentration of [³H]-WIN35,428 or [³H]-EBOB corresponding to the unbound radioactivity. The best-fit equations were determined using a least squares method.

Finally, the K_i values for *l*-menthol, GBR12909, and picrotoxin for inhibition of [³H]-WIN35,428 and [³H]-EBOB binding were determined according to Eq. (7):
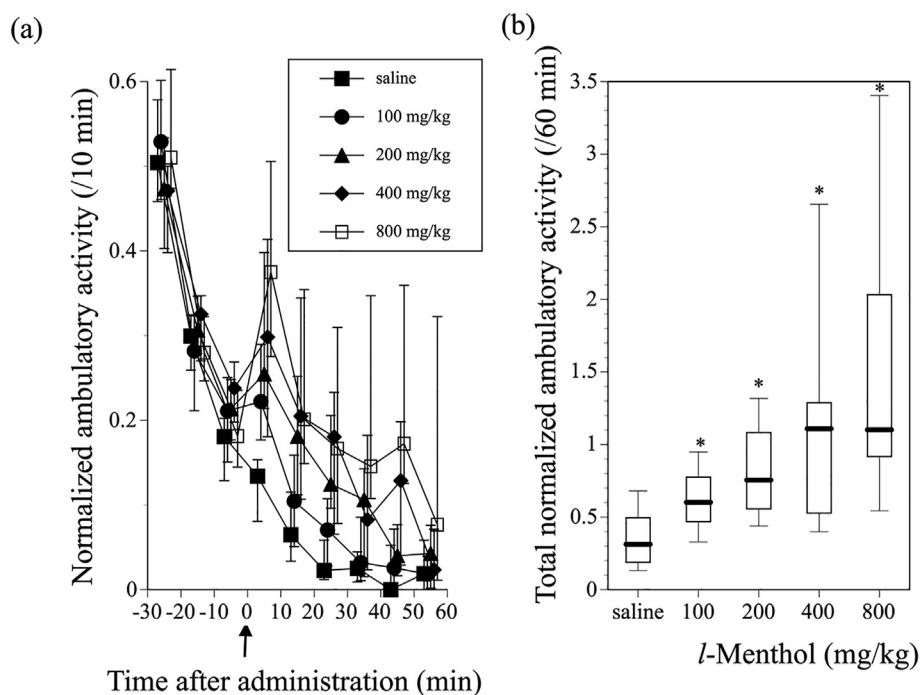
$$K_i = IC_{50} / (1 + [L / K_d]) \tag{7}$$

where L represents the concentration of [³H]-WIN35,428 or [³H]-EBOB used to determine the IC_{50} value.

3. Results

3.1. Effect of l-menthol on mouse ambulatory activity

Tilting activity cages, as used in the present study, are more sensitive to horizontal movements of mice, such as ambulation, than vertical movement, such as rearing. Following placement in the activity cages, the mice exhibited high ambulatory activity, which was followed by a decrease in activity during the 30-min adaptation period. After the adaptation period, the mice were subcutaneously administered saline or 100, 200, 400, or 800 mg/kg *l*-menthol. Significant promotion of ambulatory activity was observed following administration of *l*-menthol at all doses tested. Ambulatory activity reached a maximum 5 min after *l*-menthol administration, followed by a decrease in activity to the level of the saline-treated control mice within 60 min (Figure 1 (a)). In addition,

Figure 1. Effect of *l*-menthol on ambulatory activity in mice. (a) Change in normalized ambulatory activity before and after subcutaneous administration of vehicle or 100–800 mg/kg *l*-menthol. Symbols show median values of normalized ambulatory activity for each 10-min period plotted against the midpoint of the measurement period, and vertical lines denote the first and third quartiles. Arrow indicates the time of vehicle or 100–800 mg/kg *l*-menthol administration. (b) Total normalized ambulatory activity for 60 min after administration of vehicle or 100–800 mg/kg *l*-menthol. Data are shown using a box plot. *$P < 0.05$ compared with vehicle control (n = 19–20 mice).

the ambulation-promoting effect of *l*-menthol was dose dependent (Kruskal-Wallis test; $\chi^2{}_4 = 38.7739$, $P < 0.0001$) (Figure 1(b)).

3.2. Identification of potential target biomolecules of l-menthol

Positive control substances inhibited the binding of the isotope-labeled ligands at inhibition rates ranging from 92.7 to 100% in all assays (Tables 1, 2, and 3). This result indicated that the binding assay was suitable for evaluating the specific binding of the isotope-labeled ligands to the corresponding molecules of interest under the experimental conditions used.

At 0.1 mM, *l*-menthol inhibited the binding of [^{3}H]-spiperone to the human recombinant dopamine D4.2 receptor (inhibition rate, 28.19%); the binding of [^{3}H]-(−)-desmethoxyverapamil, a Ca channel ligand (type

L, phenylalkylamine), to rat cerebral cortex preparation (inhibition rate, 24.78%); the binding of [^{125}I]-bombesin, a non-selective bombesin receptor ligand, to rat whole-brain preparation (inhibition rate, 21.87%); the binding of [^{3}H]-CGS21680 to human recombinant adenosine A2a receptor (inhibition rate, 21.62%); the binding of [^{3}H]-tiotidine to human recombinant histamine H2 receptor (inhibition rate, 21.17%); the binding of [^{3}H]-EBOB, a GABA$_A$ receptor picrotoxin site ligand, to rat cerebral cortex preparation (inhibition rate, 20.9%); and the binding of [^{3}H]-WIN35,428 to human recombinant dopamine transporter (inhibition rate, 20.67%) (Table 1 (a)).

The same concentration (0.1 mM) of *l*-menthol also inhibited the binding of [^{125}I]-angiotensin II (Sar 1, Ile 8) to human recombinant angiotensin AT1 receptor (inhibition rate, 16.92%); the binding of [^{3}H]-batrachotoxinin A 20-alpha-benzoate, a sodium (Na) channel

Table 1. Inhibition rate (%) by *l*-menthol of binding of a ligand against a specific molecule (a) Ligands of which inhibition rate were more than 20 % (b) Ligands of which inhibition rate were more than 10 % and less than 20 %.

Molecule of interest	Radioactive isotope-labeled ligand	Preparation containing molecule of interest	Inhibition by *l*-Menthol (%)	Inhibition by a positive control substance (%)	Positive control substance
Inhibition > 20 %					
Dopamine D4.2 receptor (Human)	[3H]-Spiperone	Human recombinant	28.19	100	Haloperidol
Ca channel (Type L, Phenylalkylamine)	[3H]-(-)-Desmethoxyverapamil	Rat cerebral cortex	24.78	100	(±)-Methoxyverapamil hydrochloride
Bombesin receptor (Non-selective)	[125I]-Bombesin	Rat whole brain	21.87	98.81	Bombesin acetate hydrate
Adenosine A2a receptor (Human)	[3H]-CGS21680	Human recombinant	21.62	99.12	CGS21680 hydrochloride
Histamine H2 receptor (Human)	[3H]-Tiotidine	Human recombinant	21.17	100	Cimetidine
GABA A receptor (Picrotoxin site)	[3H]-EBOB	Rat cerebral cortex	20.9	94.33	Picrotoxin
Dopamine transporter (Human)	[3H]-WIN35,428	Human recombinant	20.67	99.41	GBR12909 dihydrochloride
(b) 20% > Inhibition > 10 %					
Angiotensin AT1 receptor (Human)	[125I]-Angiotensin II (Sar 1, Ile 8)	Human recombinant	16.92	100	Angiotensin II human
Na Channel	[3H]-Batrachotoxinin A 20-alpha-Benzoate	Rat whole brain	14.04	99.46	Dibucaine hydrochloride
Vasopressin V2 receptor (Human)	[3H]-Vasopressin, 8-L-Arginine	Human recombinant	13.53	98.02	[Arg 8]-Vasopressin
Leukotriene B4 receptor	[3H]-Leukotriene B4	Guinea pig lung	11.63	92.71	Leukotriene B4
α2A-Adrenergic receptor (Human)	[3H]-Rauwolscine hydrochloride	Human recombinant	11.34	100	Rauwolscine hydrochloride
GABA transporter	gamma-[3H]-Aminobutyric Acid, ([3H]GABA)	Rat cerebral cortex	10.09	100	γ-Aminobutyric acid (GABA)

Table 2. Inhibition rate (%) by *l*-menthol of binding of a ligand against a specific molecule. This table shows a list of ligands of which inhibition rate were more than 1 % and less than 10 %.

Molecule of interest	Radioactive isotope-labelled ligand	Preparation containing molecule of interest	Inhibition by *l*-Menthol (%)	Inhibition by a positive substance (%)	Positive substance
10% > Inhibition >1 %					
Cannabinoid CB1 receptor (Human)	[3H]-CP-55,940	Human recombinant	9.12	100	(R)-(+)-WIN55212-2 mesylate salt
Cannabinoid CB2 receptor (Human)	[3H]-CP-55,940	Human recombinant	8.57	100	(R)-(+)-WIN55212-2 mesylate salt
Serotonin 5HT2A receptor (Human)	[3H]-Ketanserin hydrochloride	Human recombinant	8.32	100	Ketanserin tartrate salt
Adenosine A3 receptor (Human)	[125I]-AB-MECA	Human recombinant	8.22	99.41	IB-MECA
Norepinephrine transporter (Human)	[3H]-Nisoxetine hydrochloride	Human recombinant	7.89	99.13	Desipramine hydrochloride
Bradykinin B2 receptor (Human)	[3H]-Bradykinin	Human recombinant	7.88	94.95	HOE140
α2C-Adrenergic receptor (Human)	[3H]-Rauwolscine hydrochloride	Human recombinant	7.75	100	Rauwolscine hydrochloride
Monoamine transporter	[3H]-α-Dihydrotetrabenazine	Rabbit platelet	7.73	100	Ketanserin tartrate salt
Imidazoline receptor (Central)	[3H]RX 781094(3H-Idazoxan)	Rat cerebral cortex	6.53	100	Guanabenz acetate salt
Dopamine D3 receptor (Human)	R-(+)-7-Hydroxy-[3H]DPAT	Human recombinant	6.32	100	(±)-7-Hydroxy-2-(di-n-propylamino)tetralin ((±)-7-OH-DPAT)
Neurokinin NK2 receptor (Human)	[3H]-SR 48968	Human recombinant	6.12	99.61	Neurokinin A
Bradykinin B1 receptor (Human)	[3H]-Kallidin (Des-Arg 10, Leu 9)	Human recombinant	6.03	100	Lys-(des-Arg 9 , Leu 8)-Bradykinin trifluoroacetate salt
Opiate ORL1 receptor (Human)	[3H]-Nociceptin	Human recombinant	5.76	100	Orphanin FQ
Melatonin MT1 receptor (Human)	[125I]-Melatonin	Human recombinant	5.74	100	Melatonin
α1A-Adrenergic receptor	[3H]-Prazosin	Rat submandibular gland	5.13	100	Prazosin hydrochloride
K channel KA	[125I]-Dendrotoxin	Rat cerebral cortex	5.11	99.78	α-Dendrotoxin
Opiate κ receptor (Human)	[3H]-Diprenorphine	Human recombinant	4.86	100	U-69593
Neurokinin NK3 receptor (Human)	[125I]-Neurokinin B (N–Me-Phe 7)	Human recombinant	4.65	100	Succinyl-[Asp 6, N–Me-Phe 8]-Substance P Fragment 6–11(Senktide)
Glutamate (NMDA polyamine site)	[3H]-Ifenprodil	Rat cerebral cortex	3.79	99.68	Ifenprodil tartrate salt
Neurokinin NK1 receptor (Human)	[125I]-Substance P	Human recombinant	3.74	99.87	L-703,606 oxalate salt hydrate
Endothelin ETB receptor (Human)	[125I]-Endothelin-1 (Human, Porcine)	Human recombinant	3.39	95.1	Endothelin-1(Human)
CCK B receptor (Human)	[125I]-Cholecystokinin Octapeptide	Human recombinant	3.31	100	CCK-Octapeptide (26–33) (Sulfated Form) (CCK-8)
α2B-Adrenergic receptor (Human)	[3H]-Rauwolscine hydrochloride	Human recombinant	2.87	100	Rauwolscine hydrochloride
Glutamate receptor (NMDAglycine site)	[3H]-MDL105,519	Rat cerebral cortex	2.56	100	MDL105,519
VIP 1 receptor (Human)	[125I]-Vasoactive Intestinal Polypeptide	Human receptor (Non-recombinant)	2.48	100	Vasoactive Intestinal Peptide human, porcine, rat (VIP)
K Channel SkCa	[125I]-Apamin	Rat whole brain	2.36	100	Apamin
Serotonin 5HT3 receptor (Human)	[3H]-GR65630	Human recombinant	2.21	95.14	MDL72222
K Channel KATP	[3H]-Glybenclamide	Rat whole brain	2.08	100	Glibenclamide
Adenosine A1 receptor (Human)	[3H]8-Cyclopentyl-1,3-dipropylxanthine ([3H]-DPCPX)	Human recombinant	1.83	96.61	8-Cyclopentyl-1,3-dipropylxanthine (DPCPX)
α1B-Adrenergic receptor	[3H]-Prazosin	Rat liver	1.76	100	Prazosin hydrochloride
GABA A receptor (Benzodiazepine site)	[3H]-Flunitrazepam	Rat whole brain	1.37	100	Diazepam
Glutamate receptor (NMDA phencycidine site)	[3H]-(+)-MK-801	Rat cerebral cortex	1.27	100	(+)-MK-801 hydrogen maleate
Ca Channel (Type L, Dihydropyridine)	[3H]-PN200-110	Rat cerebral cortex	1.17	100	Nitrendipine
GABA B receptor	gamma-[3H]-Aminobutyric Acid, ([3H]GABA)	Rat cerebellum	1.1	93.92	γ-Aminobutyric acid (GABA)

ligand, to rat whole-brain preparation (inhibition rate, 14.04%); the binding of [3H]-vasopressin (8-L-arginine) to human recombinant vasopressin V2 receptor (inhibition rate, 13.53%); the binding of [3H]-leukotriene B4, a leukotriene B4 receptor ligand, to guinea pig lung preparation (inhibition rate, 11.63%); the binding of [3H]-rauwolscine hydrochloride to human recombinant α2A-adrenergic receptor (inhibition rate, 11.34%); and the binding of [3H]-GABA, a GABA transporter ligand, to rat cerebral cortex preparation in the presence of isoguvacine hydrochloride and S (−)-baclofen hydrochloride (inhibition rate, 10.09%) (Table 1 (b)).

In addition, 0.1 mM *l*-menthol inhibited the binding of 34 different isotope-labeled ligands at an inhibition rate between 1 and 10% (Table 2). Inhibition rates for the binding of 9 isotope-labeled ligands

were <1% (Table 3 (a)). *l*-Menthol at 0.1 mM did not measurably inhibit the binding of 32 isotope-labeled ligands (Table 3 (b)).
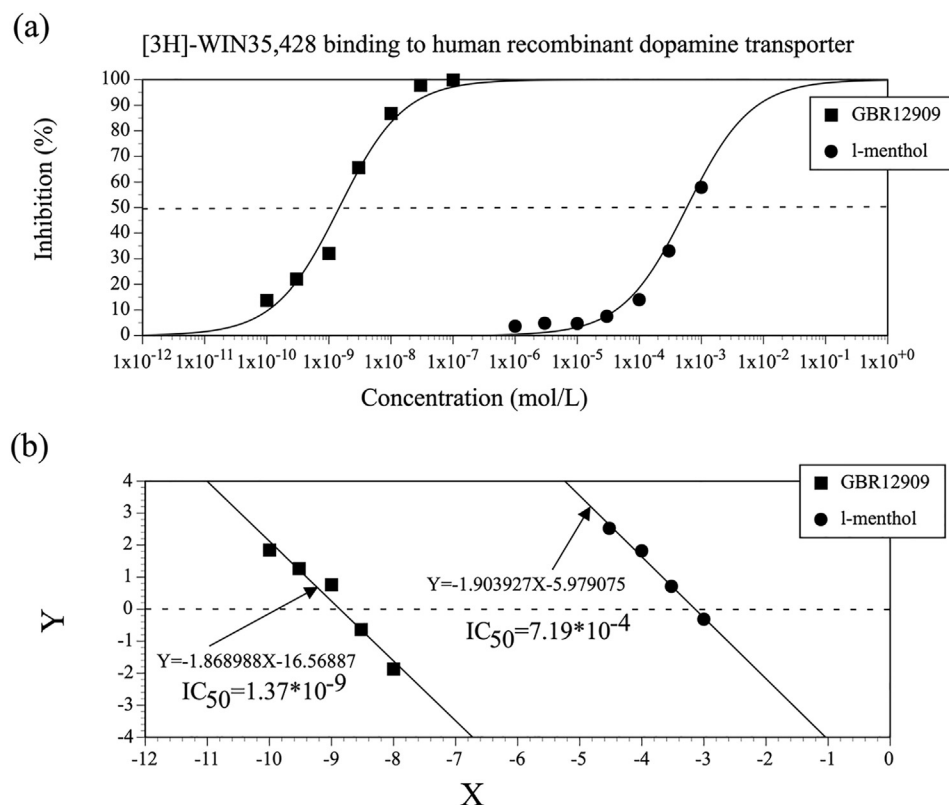
3.3. Determination of IC$_{50}$ and K$_i$ values for l-menthol–mediated inhibition of the binding of [^{3}H]-WIN35,428 and [^{3}H]-EBOB in comparison with positive control substances

Given that the dopamine transporter inhibitor bupropion synergistically interacts with menthol during mouse ambulation (Umezu and Morita, 2003), the present study also quantitatively examined *l*-menthol–mediated inhibition of the [3H]-WIN35,428 binding to determine the IC$_{50}$ and K$_i$ values, which were compared with the respective values for the positive control substance GBR12909. In addition, the present

Table 3. Inhibition rate (%) by *l*-menthol of binding of a ligand against a specific molecule (a) Ligands of which inhibition rate were more than 0 % and less than 1 %. (b) Ligands of which inhibition rate were 0 %.

Molecule of interest	Radioactive isotope-labelled ligand	Preparation containing molecule of interest	Inhibition by *l*-Menthol (%)	Inhibition by a positive substance (%)	Positive substance
(a) 1 %>Inhibition >0 %					
Neuropeptide Y1 receptor (Human)	[125I]-Peptide YY (Porcine)	Human receptor (Non-recombinant)	0.86	99.75	[Leu 31, Pro 34]-Neuropeptide Y porcine
Estrogen receptor	[3H]-Estradiol	Rat uterus	0.84	100	β-Estradiol
Adenosine transporter (Human)	[3H]-S-(p-Nitrobenzyl)-6-thioinosine (3H-NBTI)	Human Receptor	0.68	100	S-(4-Nitrobenzyl)-6-thioinosine (NBTI)
Prostanoid EP2 receptor (Human)	[3H]-Prostaglandin E2	Human recombinant	0.66	100	Prostaglandin E2
Muscarinic M2 receptor (Human)	[3H]-Scopolamine Methyl Chloride	Human recombinant	0.37	99.97	Atropine sulfate salt monohydrate
Opiate δ receptor (Human)	[3H]-Naltrindole	Human recombinant	0.3	100	Naltriben methanesulfonate hydrate
GABA A receptor (Agonist site)	[3H]-Muscimol	Rat cerebellum	0.2	99.04	Muscimol
Glutamate receptor (Kainate)	[3H]-Kainic Acid	Rat whole brain	0.14	100	Kainic acid monohydrate
IP3 receptor	D-[3H]-Inositol-1,4,5-Triphosphate	Rat cerebellum	0.12	100	D-myo-Inositol 1,4,5-trisphosphate potassium salt
(b) Inhibition = 0 %					
β1-Adrenergic receptor (Human)	[3H]-(-)-CGP-12177	Human recombinant	**0**	95.06	(±)-Propranolol hydrochloride
β2-Adrenergic receptor (Human)	[3H]-(-)-CGP-12177	Human recombinant	0	99.74	(±)-Propranolol hydrochloride
Angiotensin AT2 receptor (Human)	[125I]-CGP-42112A	Human recombinant	0	100	Angiotensin II human
Ca channel (Type L, Benzothiazepine)	[3H]-(+)-cis-Diltiazem	Rat cerebral cortex	0	96.98	(+)-cis-Diltiazem hydrochloride
Ca Channel (Type N)	[125I]-ω-Conotoxin GVIA	Rat whole brain	0	100	ω-Conotoxin GVIA
CCK A receptor (Human)	[125I]-Cholecystokinin Octapeptide	Human recombinant	0	99.47	CCK-Octapeptide (26–33) (Sulfated Form) (CCK-8)
CRF1 receptor (Human)	[125I]-Corticotropin Releasing Factor (Ovine)	Human recombinant	0	100	Urocortin human
Dopamien D1 receptor (Human)	[3H]–SCH–23390 hydrochloride	Human recombinant	0	100	R (+)–SCH–23390 hydrochroride
Dopamine D2 receptor short isoform (Human)	[3H]-Spiperone	Human recombinant	0	94.16	(+)-Butaclamol hydrochloride
Dopamine D5 receptor (Human)	[3H]SCH 23390	Human recombinant	0	98.18	R (+)–SCH–23390 hydrochloride
Endothelin ETA receptor (Human)	[125I]-Endothelin-1 (Human, Porcine)	Human recombinant	0	100	Endothelin-1(Human)
Glucocorticoid receptor (Human)	[3H]-Dexamethasone	Human recombinant	0	99.36	Dexamethasone
Glutamate receptor (AMPA)	D,L-alpha-[3H]-Amino-3-Hydroxy-Methylisoxazole-4-Propionic Acid (3H-AMPA)	Rat cerebral cortex	0	100	(S)-AMPA
Glutamate receptor (NMDA agonist site)	[3H]-CGP-39653	Rat cerebral cortex	0	100	L-Glutamic acid hydrochloride
Glycine receptor (Strychnine sensitive)	[3H]-Strychnine	Rat spinal cord	0	98.79	Strychnine
Histamine H1 receptor (Human)	[3H]-Pyrilamine	Human recombinant	0	100	Pyrilamine maleate salt
Histamine H3 receptor (Human)	N-alpha-[3H]-Methylhistamine, Dihydrochloride	Human recombinant	0	100	(R) (−)-α-Methylhistamine dihydrochloride
Leukotriene D4 receptor	[3H]-Leukotriene D4	Guinea pig lung	0	96.63	Leukotriene D4
Muscarinic M1 receptor (Human)	[3H]-Scopolamine Methyl Chloride	Human recombinant	0	99.24	Atropine sulfate salt monohydrate
Muscarinic M3 receptor (Human)	[3H]-Scopolamine Methyl Chloride	Human recombinant	0	99.82	Atropine sulfate salt monohydrate
Muscarinic M4 receptor (Human)	[3H]-Scopolamine Methyl Chloride	Human recombinant	0	100	Atropine sulfate salt monohydrate
Muscarinic M5 receptor (Human)	[3H]-Scopolamine Methyl Chloride	Human recombinant	0	99.82	Atropine sulfate salt monohydrate
Neuropeptide Y2 receptor (Human)	[125I]-Peptide YY (Human)	Human receptor (Non-recombinant)	0	98.66	Neuropeptide Y human
Neurotensin NT1 receptor (Human)	[125I]-Neurotensin	Human recombinant	0	99.56	Neurotensin
Nicotinic receptor (Human)	[3H]-(±)-Epibatidine	Human receptor (Non-recombinant)	0	100	(±)-Epibatidine dihydrochloride hydrate
Opiate μ receptor (Human)	[3H]-Diprenorphine	Human recombinant	0	100	[D-Ala 2, N–Me-Phe 4, Gly5-ol]-Enkephalin acetate salt (DAMGO)
PAF receptor	1-O-Hexadecyl-[3H]-Platelet Activating Factor (3H-PAF)	Rabbit platelet	0	100	1-O-Palmityl-sn-glycero-3-phosphocholine (PAF)
Serotonin 5HT1A receptor (Human)	[3H]-8-Hydreoxy-DPAT	Human recombinant	0	99.67	Serotonin hydrochloride
Serotonin transporter (Human)	[3H]-Imipramine hydrochloride	Human recombinant	0	96.87	Imipramine hydrochloride
Testosterone receptor (Human)	[3H]-Methyltrienolone (3H-R1881)	Human receptor	0	97.18	Testosterone
Vasopressin V1 receptor	[3H]-Vasopressin, 8-L-Arginine	Rat liver	0	98.89	[Arg 8]-Vasopressin
Vasopressin V1B receptor (Human)	[3H]-Vasopressin, 8-L-Arginine	Human recombinant	0	100	[Arg 8]-Vasopressin

(a)

(b)

Figure 2. (a) Concentration-effect relationships for *l*-menthol–mediated inhibition of the binding of [^{3}H]-WIN35,428 to the human recombinant dopamine transporter and for GBR12909. Tests were duplicated at each concentration, and data are expressed as the mean values of duplicate samples. (b) Linearized concentration-effect relationships for *l*-menthol–mediated inhibition of the [^{3}H]-WIN35,428 binding and for GBR12909, prepared using logit transformation. Y = logit y = ln (y/1 − y); y = (B–N)/(B$_0$–N); B = the amount of radioactivity bound in the presence of the test compound, B$_0$ = the amount of radioactivity bound in the absence of the test compound, N = the amount of radioactivity nonspecifically bound; X = log x; x = the concentration of *l*-menthol or positive control substance.

study determined the IC$_{50}$ and K$_i$ values for the ability of *l*-menthol and another positive control substance, picrotoxin, to inhibit the [^{3}H]-EBOB binding, as menthol has been shown to inhibit GABA$_A$ receptor activity (Oz et al., 2017).

Figure 2 shows the concentration-effect relationships for *l*-menthol–mediated inhibition of the [^{3}H]-WIN35,428 binding and for the positive control, GBR12909. The IC$_{50}$ values for *l*-menthol and GBR12909 were 7.19×10^{-4} mol/L and 1.37×10^{-9} mol/L, respectively. Concentration-effect relationships for *l*-menthol–mediated inhibition of the [^{3}H]-EBOB binding and for picrotoxin were also examined (Figure 3), with corresponding IC$_{50}$ values of 5.54×10^{-4} mol/L for *l*-menthol and 6.02×10^{-7} mol/L for picrotoxin. K$_d$ and B$_{max}$ values were determined from the concentration-effect relationships for the [^{3}H]-WIN35,428 binding and for the [^{3}H]-EBOB binding, as shown in Table 4. Based upon the IC$_{50}$ and K$_d$ values, the K$_i$ values for *l*-menthol–mediated inhibition of the [^{3}H]-WIN35,428 binding and for GBR12909 were determined and are shown in Table 5. K$_i$ values for *l*-menthol–mediated inhibition of the [^{3}H]-EBOB binding and for picrotoxin were also determined (Table 5).

Collectively, the data described above revealed that *l*-menthol inhibits the [^{3}H]-WIN35,428 binding and the [^{3}H]-EBOB binding in a concentration-dependent manner with similar K$_i$ values.
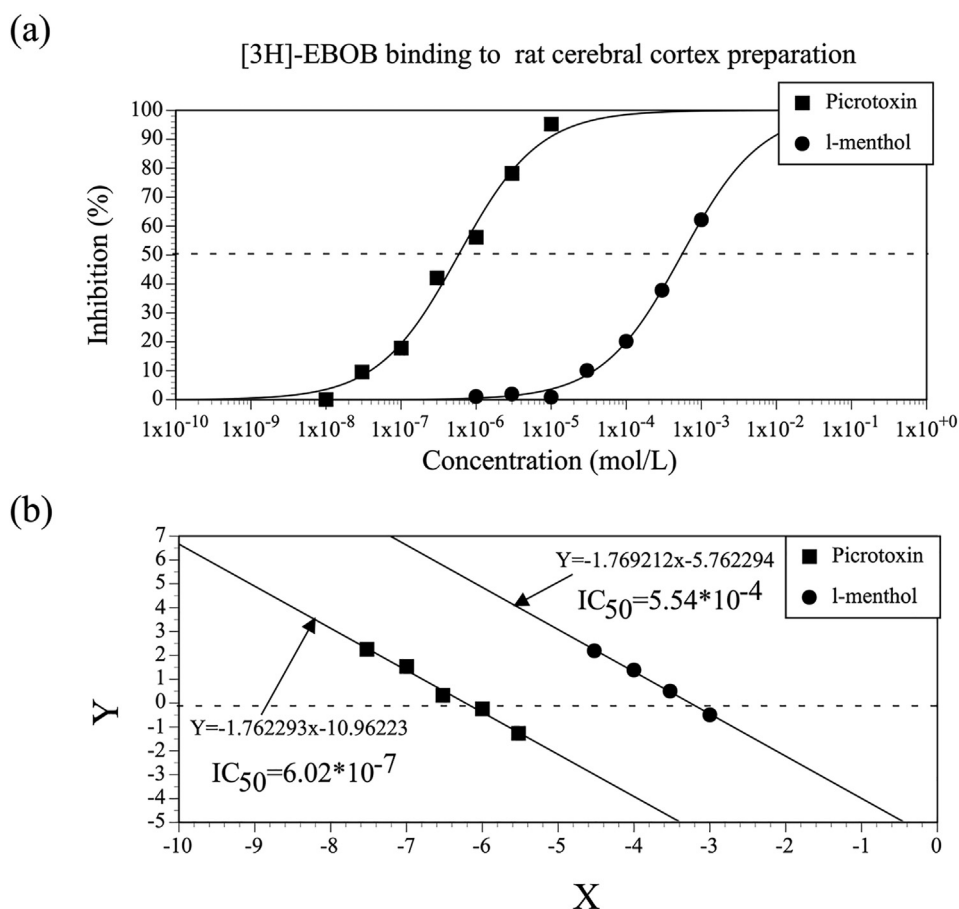
4. Discussion

Given that menthol exerts a variety of physiologic and pharmacologic effects, including CNS effects, I hypothesized that *l*-menthol would affect a variety of biomolecules at pharmacologically relevant concentrations. In particular, I was interested in identifying biomolecules involved in the ambulation-promoting effect of *l*-menthol. Consistent with previously reported findings (Oz et al., 2017), the present study found that *l*-menthol affects Ca and Na channels as wells as the GABA$_A$ receptor. Furthermore, the results of the present study suggest that *l*-menthol affects the GABA transporter, the dopamine D4.2 receptor, the dopamine transporter, the adenosine A2a receptor, the α2A-adrenergic receptor, the histamine H2 receptor, the bombesin receptor, the

angiotensin AT1 receptor, the vasopressin V2 receptor, and the leukotriene B4 receptor.

The striatum plays an important role in controlling mouse locomotion. Medium spiny neurons mediate output from the striatum, with GABA functioning as the neurotransmitter (Hikida et al., 2010). GABA neurons in the ventral tegmental area and raphe nucleus also play a role in controlling locomotion (Arnt and Scheelkruger, 1979; Shim et al., 2014). One study examining recombinant human GABA$_A$ receptor expressed in *Xenopus* oocytes suggested that *l*-menthol acts as a positive allosteric modulator of the GABA$_A$ receptor rather than an agonist (Hall et al., 2004). In periaqueductal grey neurons in rat midbrain slices, *l*-menthol was shown to prolong spontaneous GABA$_A$ receptor–mediated inhibitory current, most likely via a mechanism distinct from that of benzodiazepines (Lau et al., 2014). Consistent with these findings, in the present study, *l*-menthol inhibited the [^{3}H]-EBOB binding, although the potency of *l*-menthol to inhibit the binding of [^{3}H]-muscimol, a GABA$_A$ receptor agonist ligand, and [^{3}H]-flunitrazepam, a GABA$_A$ receptor benzodiazepine ligand, was very low. It should be noted that barbiturates inhibit the binding of picrotoxin to the GABA$_A$ receptor and enhance GABA$_A$ receptor–mediated inhibitory currents (Olsen, 2014). In periaqueductal grey neurons, *l*-menthol also enhances tonic GABA$_A$ receptor–mediated currents, which are thought to require the continual presence of low levels of extracellular GABA (Semyanov et al., 2004). The *l*-menthol–mediated enhancement of tonic GABA$_A$ receptor–mediated currents is tetrodotoxin insensitive (Lau et al., 2014). The effect of *l*-menthol on the GABA transporter as suggested by the results of the present study could play a role in the enhancement of tonic GABA$_A$ receptor–mediated currents. Although the present study provides further evidence that *l*-menthol affects GABAergic neurotransmission, it should be noted that GABA$_A$ agonists, barbiturates, and benzodiazepines cause sedation in rodents. The precise role of GABAergic neurotransmission in the ambulation-promoting effect of *l*-menthol thus remains to be elucidated.

The results of the present study suggest that *l*-menthol acts on the dopamine D4 receptor and the dopamine transporter. Although data regarding the role of the dopamine D4 receptor in the CNS remain

(a)

(b)

Figure 3. (a) Concentration-effect relationships for *l*-menthol–mediated inhibition of the binding of [³H]-EBOB, a GABA$_A$ receptor picrotoxin ligand, to rat cerebral cortex preparation and for picrotoxin. Tests were duplicated at each concentration, and data are expressed as the mean values of duplicate samples. (b) Linearized concentration-effect relationships for *l*-menthol–mediated inhibition of the [³H]-EBOB binding and for picrotoxin, prepared using logit transformation.

Table 4. K$_d$ and B$_{max}$ values for the binding of [³H]-WIN35,428 and [³H]-EBOB.

Radioactive isotope-labelled ligand	Molecule of interest	K$_d$ (nmol/L)	B$_{max}$ (fmol/mg)
[³H]-WIN35,428	Dopamine transporter (Human)	13.9	17668.63
[³H]-EBOB	GABA$_A$ (Picrotoxin site)	4.18	11.96

Table 5. K$_i$ values of *l*-menthol and positive control substances for inhibition of the binding of [³H]-WIN35,428 and [³H]-EBOB.

Radioactive isotope-labelled ligand	Molecule of interest	Substance	K$_i$ (mol/L)
[³H]-WIN35,428	Dopamine transporter (Human)	*l*-Menthol	6.15×10^{-4}
		GBR12909	1.17×10^{-9}
[³H]-EBOB	GABA$_A$ (Picrotoxin site)	*l*-Menthol	2.88×10^{-4}
		Picrotoxin	3.13×10^{-7}

limited, a lack of dopamine D4 receptor is known to cause supersensitivity to the locomotion-increasing effects of ethanol, cocaine, and methamphetamine in mice (Rubinstein et al., 1997). It is thus possible that effects on the dopamine D4 receptor play a role in the ambulation-promoting effect of *l*-menthol. The dopamine transporter reuptakes dopamine released from the synaptic cleft and thus plays an important role in maintaining dopamine homeostasis. Bupropion inhibits the dopamine transporter, resulting in increased extracellular dopamine levels and neuronal activity in the striatum, thus promoting mouse ambulation (Umezu and Shibata, 2016). In the human dopamine

transporter, the binding sites for [³H]-WIN35,428 exhibit pharmacologic identity with the dopamine uptake and/or binding sites (Pristupa et al., 1994; Sun et al., 2019). GBR12909 binds to the piperazine acceptor site of the dopamine transporter to inhibit [³H]-WIN35,428 binding and dopamine uptake (Andersen et al., 1987; Sun et al., 2019). The results of the present study demonstrated that *l*-menthol inhibits the [³H]-WIN35,428 binding, similar to GBR12909, suggesting that *l*-menthol inhibits the binding of dopamine to the dopamine transporter and leading to decreased dopamine uptake. How *l*-menthol inhibits the [³H]-WIN35,428 binding remains unclear. However, it is possible that *l*-menthol interacts with bupropion on the dopamine transporter, and this interaction could play a role in the synergistic interaction between *l*-menthol and bupropion in promoting mouse ambulation (Umezu and Morita, 2003).

The ambulation-promoting effects of scopolamine, MK-801, morphine, and caffeine (Kuribara, 1997; Kuribara et al., 1992; Umezu, 2013) suggest that muscarinic cholinergic receptors, NMDA-type glutamate receptors, opiate μ-type receptors, and adenosine type A2a receptors are also involved in mouse ambulation. The results of the present study suggest that *l*-menthol affects muscarinic cholinergic receptors, NMDA-type glutamate receptors, and opiate μ-type receptors with very low potency. In contrast, my results also suggest that *l*-menthol affects the

adenosine A2a receptor. The chemical structure of *l*-menthol suggests that it does not function as an agonist to the adenosine A2a receptor, as the adenosine scaffold is necessary as a structural basis for agonists (Ruiz et al., 2014). Adenosine A2a receptors are highly expressed in the dopamine-rich regions of the brain. The motor-stimulating effect of caffeine is produced via antagonism of adenosine A2a receptors expressed in the medium spiny neurons in the striatum through a dopamine-dependent mechanism (Fisone et al., 2004). Accordingly, the adenosine A2a receptor may also play a role in the ambulation-promoting effect of *l*-menthol. As the adenosine A2a receptor is expressed in a variety of tissues and organs throughout the body in addition to the CNS, *l*-menthol may also affect blood pressure and heart rate, wound repair, repair and generation of connective tissues, control of cytokine release in the sympathetic nervous system, and initiation and termination of inflammation in the lungs (Ruiz et al., 2014).

The results of the present study suggest that *l*-menthol also affects the α2A-adrenergic receptor. Given that the α2A-adrenergic receptor is known to play a role in controlling locomotion (Juhila et al., 2005), it may also be involved in the ambulatory effect of *l*-menthol. In addition, *l*-menthol was shown to affect mood, emotions, blood pressure, and sympathetic nervous system activity via the α2A-adrenergic receptor (Schramm et al., 2001; MacMillan et al., 1996; Hein et al., 1999). The present results also suggest that *l*-menthol affects the histamine H2 receptor, the bombesin receptor, the angiotensin AT1 receptor, the vasopressin V2 receptor, and the leukotriene B4 receptor. Although whether these molecules play a role in mouse ambulation remains unclear, *l*-menthol may exert some pharmacologic effects via these receptors.

The histamine H2 receptor is thought to play roles in relaxation of the airway and vascular smooth muscles, regulation of cardiac muscle activity, chemotactic responses of basophils, induction of suppressor T cells, inhibition of mitogen-mediated immunocyte proliferation, regulation of gastric acid secretion, and intestinal secretion (DelValle and Gantz, 1997). Three different bombesin receptors have been identified and found to be widely distributed in the CNS and peripheral tissues. These receptors are involved in satiety, regulation of energy balance and metabolism, contraction and motility of the gastrointestinal tract, lung development and lung diseases, thermoregulation, and immune cell function and pruritus (Gonzalez et al., 2008). The renin-angiotensin-aldosterone system plays an important role in cardiovascular and renal physiology and pathophysiology, including regulation of salt and water balance, vasoconstriction, and cardiovascular dysfunction. Angiotensin plays a major role in this system, and many of its effects are mediated via the angiotensin AT1 receptor (Kawai et al., 2017). Vasopressin is an antidiuretic hormone, and vasopressin V2 receptor antagonists are used clinically as diuretics (Ranieri et al., 2020). Leukotriene B4, a potent chemotactic factor and activator of neutrophils and macrophages, is thought to play roles in various inflammatory diseases, such as rheumatoid arthritis, asthma, and chronic obstructive pulmonary disease (Bhatt et al., 2017). Although the effect of *l*-menthol on these biomolecules remains to be investigated in future research, it is noteworthy that menthol has been used in traditional treatments for respiratory diseases, gastrointestinal disorders, the common cold, and musculoskeletal pain, and also as an antipruritic (Lau et al., 2014; Oz et al., 2017).

In conclusion, the results of the present study demonstrated that *l*-menthol inhibits the binding of 13 different ligands to specific biomolecules at relatively high inhibition rates. The present results suggest that the dopamine transporter, adenosine A2a receptor, dopamine D4 receptor, α2A-adrenergic receptor, and GABA$_A$ receptor are promising candidate molecules for future research into the mechanism underlying the psychostimulant-like effect of *l*-menthol on mouse locomotion.

Declarations

Author contribution statement

Toyoshi Umezu: Conceived and designed the experiments; Performed the experiments; Analyzed and interpreted the data; Wrote the paper.

Data availability statement

Data included in article/supplementary material/referenced in article.

Declaration of interests statement

The authors declare no conflict of interest.

Additional information

Supplementary content related to this article has been published online at https://doi.org/10.1016/j.heliyon.2021.e07329.

References

Alsharari, S.D., King, J.R., Nordman, J.C., Muldoon, P.P., Jackson, A., Zhu, A.Z.X., Tyndale, R.F., Kabbani, N., Damaj, M.I., 2015. Effects of menthol on nicotine pharmacokinetic, pharmacology and dependence in mice. PloS One 10 (9), e0137070.

Amato, A., Serio, R., Mule, F., 2014. Involvement of cholinergic nicotinic receptors in the menthol-induced gastric relaxation. Eur. J. Pharmacol. 745, 129–134.

Andersen, P.H., Jansen, J.A., Nielsen, E.B., 1987. [3H]GBR 12935 binding in vivo in mouse brain: labelling of a piperazine acceptor site. Eur. J. Pharmacol. 144, 1–6.

Arnt, J., Scheelkruger, J., 1979. GABA in the ventral tegmental area - differential regional effects on locomotion, aggression and food-intake after micro-injection of GABA agonists and antagonists. Life Sci. 25, 1351–1360.

Ashoor, A., Nordman, J.C., Veltri, D., Yang, K.H.S., Shuba, Y., Al Kury, L., Sadek, B., Howarth, F.C., Shehu, A., Kabbani, N., Oz, M., 2013. Menthol inhibits 5-HT3 receptor-mediated current. J. Pharmacol. Exp. Therapeut. 34, 398–409.

Bhatt, L., Roinestad, K., Van, T., Springman, E.B., 2017. Recent advances in clinical development of leukotriene B4 pathway drugs. Semin. Immunol. 33, 65–73.

Cheang, W.S., Lam, M.Y., Wong, W.T., Tian, X.Y., Lau, C.W., Zhu, Z.M., Yao, X.Q., Huang, Y., 2013. Menthol relaxes rat aortae, mesenteric and coronary arteries by inhibiting calcium influx. Eur. J. Pharmacol. 702, 79–84.

DelValle, J., Gantz, I., 1997. Novel insights into histamine H-2 receptor biology. Am. J. Physiol. Gastrointest. Liver Physiol. 273, G987–G996.

Eccles, R., 1994. Menthol and related cooling compounds. J. Pharm. Pharmacol. 46, 618–630.

Fisone, G., Borgkvist, A., Usiello, A., 2004. Caffeine as a psychomotor stimulant: mechanism of action. Cell. Mol. Life Sci. 61, 857–872.

Gaudioso, C., Hao, J.Z., Martin-Eauclaire, M.F., Gabriac, M., Delmas, P., 2012. Menthol pain relief through cumulative inactivation of voltage-gated sodium channels. Pain 153, 473–484.

Gonzalez, N., Moody, T.W., Igarashi, H., Ito, T., Jensen, R.T., 2008. Bombesin-related peptides and their receptors: recent advances in their role in physiology and disease states. Curr. Opin. Endocrinol. Diabetes Obes. 15, 58–64.

Haeseler, G., Maue, D., Grosskreutz, J., Bufler, J., Nentwig, B., Piepenbrock, S., Dengler, R., Leuwer, M., 2002. Voltage-dependent block of neuronal and skeletal muscle sodium channels by thymol and menthol. Eur. J. Anaesthesiol. 19, 571–579.

Hall, A.C., Turcotte, C.M., Betts, B.A., Yeung, W.Y., Agyeman, A.S., Burk, L.A., 2004. Modulation of human GABA(A) and glycine receptor currents by menthol and related monoterpenoids. Eur. J. Pharmacol. 506, 9–16.

Heimes, K., Hauk, F., Verspohl, E.J., 2011. Mode of action of peppermint oil and (−)-menthol with respect to 5-HT3 receptor subtypes: binding studies, cation uptake by receptor channels and contraction of isolated rat ileum. Phytother Res. 25, 702–708.

Hein, L., Altman, J.D., Kobilka, B.K., 1999. Two functionally distinct alpha(2)-adrenergic receptors regulate sympathetic neurotransmission. Nature 402, 181–184.

Henderson, B.J., Wall, T.R., Henley, B.M., Kim, C.H., Nichols, W.A., Moaddel, R., Xiao, C., Lester, H.A., 2016. Menthol alone upregulates midbrain nAChRs, alters nAChR subtype stoichiometry, alters dopamine neuron firing frequency, and prevents nicotine reward. J. Neurosci. 36, 2957–2974.

Henderson, B.J., Wall, T.R., Henley, B.M., Kim, C.H., McKinney, S., Lester, H.A., 2017. Menthol enhances nicotine reward-related behavior by potentiating nicotine-induced changes in nAChR function, nAChR upregulation, and DA neuron excitability. Neuropsychopharmacology 42, 2285–2291.

Hikida, T., Kimura, K., Wada, N., Funabiki, K., Nakanishi, S., 2010. Distinct roles of synaptic transmission in direct and indirect striatal pathways to reward and aversive behavior. Neuron 66, 896–907.

Ito, S., Kume, H., Shiraki, A., Kondo, M., Makino, Y., Kamiya, K., Hasegawa, Y., 2008. Inhibition by the cold receptor agonists menthol and icilin of airway smooth muscle contraction. Pulm. Pharmacol. Therapeut. 21, 812–817.

Juhila, J., Honkanen, A., Sallinen, J., Haapalinna, A., Korpi, E.R., Scheinin, M., 2005. Alpha(2A)-adrenoceptors regulate d-amphetamine-induced hyperactivity and behavioural sensitization in mice. Eur. J. Pharmacol. 517, 74–83.

Kaserer, T., Steinacher, T., Kainhofer, R., Erli, F., Sturm, S., Waltenberger, B., Schuster, D., Spetea, M., 2020. Identification and characterization of plant-derived alkaloids, corydine and corydaline, as novel mu opioid receptor agonists. Sci. Rep. 10, 13804.

Kawai, T., Forrester, S.J., O'Brien, S., Baggett, A., Rizzo, V., Eguchi, S., 2017. AT1 receptor signaling pathways in the cardiovascular system. Pharmacol. Res. 125 (Pt A), 4–13.

Kuribara, H., 1997. Induction of sensitization to hyperactivity caused by morphine in mice: effects of post-drug environments. Pharmacol. Biochem. Behav. 57, 341–346.

Kuribara, H., Asami, T., Ida, I., Iijima, Y., Tadokoro, S., 1992. Effects of repeated MK-801 on ambulation in mice and in sensitization following methamphetamine. Psychopharmacology 108, 271–275.

Lau, B.K., Karim, S., Goodchild, A.K., Vaughan, C.W., Drew, G.M., 2014. Menthol enhances phasic and tonic GABA(A) receptor-mediated currents in midbrain periaqueductal grey neurons. Br. J. Pharmacol. 171, 2803–2813.

Lever, S.Z., Fan, K.-H., Lever, J.R., 2017. Tactics for preclinical validation of receptor-binding radiotracers. Nucl. Med. Biol. 44, 4–30.

MacMillan, L.B., Hein, L., Smith, M.S., Piascik, M.T., Limbird, L.E., 1996. Central hypotensive effects of the alpha(2a)-adrenergic receptor subtype. Science 273, 801–803.

McKemy, D.D., Neuhausser, W.M., Julius, D., 2002. Identification of a cold receptor reveals a general role for TRP channels in thermosensation. Nature 416, 52–58.

Mollica, A., Pelliccia, S., Famiglini, V., Stefanucci, A., Macedonio, G., Chiavaroli, A., Orlando, G., Brunetti, L., Ferrante, C., Pieretti, S., Novellino, E., Benyhe, S., Zador, F., Erdei, A., Szucs, E., Samavati, R., Dvrorasko, S., Tomboly, C., Ragno, R., Patsilinakos, A., Silvestri, R., 2017. Exploring the first Rimonabant analog-opioid peptide hybrid compound, as bivalent ligand for CB1 and opioid receptors. J. Enzym. Inhib. Med. Chem. 32, 444–451.

Olsen, R.W., 2014. Analysis of gamma-aminobutyric acid (GABA) type A receptor subtypes using isosteric and allosteric ligands. Neurochem. Res. 39, 1924–1941.

Oz, M., El Nebrisi, E.G., Yang, K.-H.S., Howarth, F.C., Al Kury, L.T., 2017. Cellular and molecular targets of menthol actions. Front. Pharmacol. 8, 472.

Pan, R., Tian, Y.Z., Gao, R., Li, H.T., Zhao, X.G., Barrett, J.E., Hu, H.J., 2012. Central mechanisms of menthol-induced analgesia. J. Pharmacol. Exp. Therapeut. 343, 661–672.

Patel, T., Ishiuji, Y., Yosipovitch, G., 2007. Menthol: a refreshing look at this ancient compound. J. Am. Acad. Dermatol. 57, 873–878.

Peier, A.M., Moqrich, A., Hergarden, A.C., Reeve, A.J., Andersson, D.A., Story, G.M., Earley, T.J., Dragoni, I., McIntyre, P., Bevan, S., Patapoutian, A., 2002. A TRP channel that senses cold stimuli and menthol. Cell 108, 705–715.

Pristupa, Z.B., Wilson, J.M., Hoffman, B.J., Kish, S.J., Niznik, H.B., 1994. Pharmacological heterogeneity of the cloned and native human dopamine transporter: disassociation of [3H]WIN 35,428 and [3H]GBR 12,935 binding. Mol. Pharmacol. 45, 125–135.

Ranieri, M., Venneri, M., Pellegrino, T., Centrone, M., Di Mise, A., Cotecchia, S., Tamma, G., Valenti, G., 2020. The vasopressin receptor 2 mutant R137L linked to the nephrogenic syndrome of inappropriate antidiuresis (NSIAD) signals through an alternative pathway that increases AQP2 membrane targeting independently of S256 phosphorylation. Cells 9, 1354. Article ID.

Rubinstein, M., Phillips, T.J., Bunzow, J.R., Falzone, T.L., Dziewczapolski, G., Zhang, G., Fang, Y., Larson, J.L., McDougall, J.A., Chester, J.A., Saez, C., Pugsley, T.A., Gershanik, O., Low, M.J., Grandy, D.K., 1997. Mice lacking dopamine D4 receptors are supersensitive to ethanol, cocaine, and methamphetamine. Cell 90, 991–1001.

Ruiz, M.D., Lim, Y.H., Zheng, J.Y., 2014. Adenosine A(2a) receptor as a drug discovery target. J. Med. Chem. 57, 3623–3650.

Schramm, N.L., McDonald, M.P., Limbird, L.E., 2001. The alpha(2A)-adrenergic receptor plays a protective role in mouse behavioral models of depression and anxiety. J. Neurosci. 21, 4875–4882.

Semyanov, A., Walker, M.C., Kullmann, D.M., Silver, R.A., 2004. Tonically active GABA(A) receptors: modulating gain and maintaining the tone. Trends Neurosci. 27, 262–269.

Shim, I., Stratford, T.R., Wirtshafter, D., 2014. Dopamine is differentially involved in the locomotor hyperactivity produced by manipulations of opioid, GABA and glutamate receptors in the median raphe nucleus. Behav. Brain Res. 261, 65–70.

Sun, W.L., Quizon, P.M., Yuan, Y.X., Strauss, M.J., McCain, R., Zhan, C.G., Zhu, J., 2019. Mutational effects of human dopamine transporter at tyrosine88, lysine92, and histidine547 on basal and HIV-1 Tat-inhibited dopamine transport. Sci. Rep. 9, 3843. Article ID.

Swandulla, D., Schafer, K., Lux, H.D., 1986. Calcium-channel current inactivation is selectively modulated by menthol. Neurosci. Lett. 68, 23–28.

Swandulla, D., Carbone, E., Schafer, K., Lux, H.D., 1987. Effect of menthol on 2 types of Ca currents in cultured sensory neurons of vertebrates. Pflügers Archiv 409, 52–59.

Tani, M., Onimaru, H., Ikeda, K., Kawakami, K., Homma, I., 2010. Menthol inhibits the respiratory rhythm in brainstem preparations of the newborn rats. Neuroreport 21, 1095–1099.

Thompson, M.F., Poirier, G.L., Davila-Garcia, M.I., Huang, W., Tam, K., Robidoux, M., Dubuke, M.L., Shaffer, S.A., Colon-Perez, L., Febo, M., DiFranza, J.R., King, J.A., 2018. Menthol enhances nicotine-induced locomotor sensitization and in vivo functional connectivity in adolescence. J. Psychopharm. 32, 332–343.

Umezu, T., Sakata, A., Ito, H., 2001. Ambulation-promoting effect of peppermint oil and identification of its active constituents. Pharmacol. Biochem. Behav. 69, 383–390.

Umezu, T., Morita, M., 2003. Evidence for the involvement of dopamine in ambulation promoted by menthol in mice. J. Pharmacol. Sci. 91, 125–135.

Umezu, T., 2012. Unusual Effects of nicotine as a psychostimulant on ambulatory activity in mice. ISRN Pharmacol. 2012, 170981. Article ID.

Umezu, T., 2013. Evaluation of central nervous system acting effects of plant-derived essential oils using ambulatory activity in mice. Pharmacol. Pharm. 4, 160–170.

Umezu, T., Shibata, Y., 2016. Brain regions and monoaminergic neurotransmitters that are involved in mouse ambulatory activity promoted by bupropion. Toxicol. Rep. 3, 552–562.

Zhang, X.B., Jiang, P., Gong, N., Hu, X.L., Fei, D., Xiong, Z.Q., Xu, L., Xu, T.L., 2008. A-type GABA receptor as a central target of TRPM8 agonist menthol. PloS One 3, e3386. Article ID.